Dimethyl Methylphosphonate Decomposition on Titania-Supported Ni Clusters and Films: A Comparison of Chemical Activity on Different Ni Surfaces

J. Zhou, S. Ma, Y. C. Kang,† and D. A. Chen*

Department of Chemistry and Biochemistry, University of South Carolina, Columbia, South Carolina 29208

Received: February 27, 2004; In Final Form: May 11, 2004

The thermal decomposition of dimethyl methylphosphonate (DMMP) has been studied in ultrahigh vacuum by temperature programmed desorption (TPD) and X-ray photoelectron spectroscopy (XPS) on Ni clusters and films deposited on TiO_2(110). The four different Ni surfaces under investigation consisted of small Ni clusters (5.0 ± 0.8 nm diameter, 0.9 ± 0.2 nm height) deposited at room temperature and quickly heated to 550 K, large Ni clusters (8.8 ± 1.4 nm diameter, 2.3 ± 0.5 nm height) prepared by annealing to 850 K, a 50 monolayer Ni film deposited at room temperature, and a 50 monolayer Ni film annealed to 850 K. The morphologies of the Ni surfaces were characterized by scanning tunneling microscopy (STM). TPD experiments show that CO and H_2 are the major gaseous products evolved from the decomposition of DMMP on all of the Ni surfaces, and molecular DMMP and methane desorption were also observed. The product yields for CO and H_2 were highest for reactions on the small Ni clusters and unannealed Ni film and lowest for reactions on the large clusters and annealed film. Furthermore, XPS experiments demonstrate that the unannealed Ni surfaces decompose a greater fraction of DMMP at room temperature. The loss of activity for the annealed surfaces is not caused by a reduction in surface area because the annealed surfaces have approximately the same surface area as the small clusters. CO adsorption studies suggest that the loss of activity upon annealing cannot be completely due to a decrease in surface defects, such as step and edge sites, and we propose that a TiO_x moiety is responsible for blocking active sites on the annealed Ni surfaces. In comparison to the TiO_2 surface, the small Ni clusters are more chemically active because a greater fraction of DMMP decomposes at room temperature, and the total amount of DMMP decomposition is also higher on the small Ni clusters. Although DMMP decomposes on TiO_2 to produce gaseous methyl radicals, methane, and H_2, the activity of the substrate surface itself appears to be quenched in the presence of the Ni clusters and films. However, the TiO_2 support plays a significant role in providing a source of oxygen for the recombination of atomic carbon on Ni to form CO, which desorbs above 800 K.

Introduction

Dimethyl methylphosphonate (DMMP) is frequently used as a simulant for probing the reactivity of toxic organophosphorus compounds, which are used in chemical warfare agents as well as in herbicides and insecticides. The development of methods for destroying chemical warfare agents has become an increasingly important area of research.[1,2] Specific emphasis has been placed on techniques to provide protection from exposure to chemical warfare agents as well as for the destruction of stockpiles of chemical weapons. There is clearly a need for the development and design of new materials that can irreversibly decompose chemical agents and convert them into a nontoxic form. Activated carbon sorbents are currently used in standard protection equipment such as combat suits and the Army's M-40 series masks. However, the efficiency of carbon sorbents for removing toxic compounds from the air is not ideal because physical adsorption of the chemical agents is a reversible and nonselective process. Many of these problems can be avoided by employing materials that remove chemical agents via decomposition rather than adsorption. Supported metal nanoparticles represent a new class of materials that can potentially be incorporated into air filtration systems and sorbents for decontamination.

Heterogeneous catalysis has already shown promise as a route for the decomposition of chemical warfare agents. Previous studies of DMMP on bulk transition metal surfaces have demonstrated that reactions on these surfaces facilitate decomposition either into atomic carbon and oxygen or into small, less toxic molecules such as CO, CO_2, and methanol; phosphorus is also deposited on the surface.[2−4] The major obstacle to catalytic reaction on these surfaces is that the atomic decomposition products poison active sites. Although studies on Mo(110) and Pd(111) have shown that reactivity can be sustained by removing phosphorus from the surface via continuous oxidation, relatively high temperatures (900−1075 K) were required.[5,6] Only a fraction of the phosphorus can be removed from Pd even at temperatures of 950 K, and phosphorus cannot be oxidized on Ni(111).[6] The key to sustained chemical activity is that the surface must be reactive enough to break P−O, P−C, and S−C bonds but not so reactive that atomic byproducts cannot be easily removed. In general, this reactivity balance is difficult to achieve on bulk transition metal surfaces.

Supported metal nanoparticles have the potential to exhibit new surface chemistry compared to their bulk metal counterparts. Furthermore, it may be possible to control the reactivity of nanoparticle surfaces by systematically changing the physical

* Corresponding author. Phone: 803-777-1050. Fax: 803-777-9521. E-mail: chen@mail.chem.sc.edu.

† Current address: Department of Chemistry, Pukyong National University, South Korea.

10.1021/jp040185m CCC: $27.50
Published on Web 07/02/2004

and electronic properties of these particles. Not only do nanoparticles provide greater surface area on which reaction can occur, but their reactivities can be remarkably different from that of the bulk material. Haruta and co-workers' studies of supported Au particles are the classic example used to demonstrate the unusual activity of supported metal nanoparticles.[7−9] Although bulk Au surfaces are chemically inert, Au nanoparticles on titania are active materials for reactions such as CO hydrogenation,[10] CO oxidation,[11,12] epoxidation of propylene,[13] and the water gas shift reaction.[14] A number of other studies in the catalysis literature have demonstrated that chemistry on the supported metal particles can depend on their size and structure,[15−22] but the details of this relationship are still not fully understood; to date, there have been few investigations of metal nanoparticles that address their surface chemistry on the atomic level.

In this work, we have studied the decomposition of DMMP on Ni particles and films deposited on TiO_2(110)-(1 × 1). The Ni surfaces were characterized by scanning tunneling microscopy, and the chemistry of DMMP on these surfaces was investigated by temperature programmed desorption (TPD) and X-ray photoelectron spectroscopy (XPS). Single-crystal rutile TiO_2 acts as an ideal support surface because the (110) face has a well-defined structure as well as good thermal stability and the titania can be made conductive enough for STM and XPS experiments by heating in vacuum to reduce the crystal. Although transition metal surfaces have shown promise as catalysts for the decomposition of organophosphorus compounds, there have been few detailed studies of these reactions on supported metal nanoparticles. Ni was chosen for these investigations for the following reasons. First, the growth of Ni particles on TiO_2(110) of various sizes with uniform size distributions has been well studied by microscopy techniques.[23,24] Second, because the chemistry of DMMP on the Ni(111) surface is known,[6] the reactivity of the Ni particles can be compared to that of a known and well-defined surface structure. The Ni particles may have enhanced reactivity due to unique structures that are not observed on bulk surfaces or due to a greater number of defects sites, such as steps, kinks, vacancies, or any other higher coordination sites. A number of chemical reactions, such as hydrogenation,[25,26] hydrogenolysis,[25,26] desulfurization,[27] and hydrodechlorination,[18] are known to be sensitive to the structure of the Ni surfaces. Third, interactions between Ni and the TiO_2 support are known to exist[28,29] but are not as strong as the interactions with transition metals such as Fe[30,31] and Cr,[32] which reduce the TiO_2 surface upon deposition in ultrahigh vacuum.[33,34] Therefore, it is possible that the TiO_2 support could play a role in oxidizing carbon or phosphorus from the surfaces of the Ni particles to prevent passivation.

DMMP chemistry was investigated on the following five surfaces: TiO_2(110)-(1 × 1); a 3 ML Ni coverage on TiO_2 heated to 550 K to produce clusters 5.0 ± 0.8 nm in diameter and 0.9 ± 0.2 nm in height; an 8 ML Ni coverage heated to 850 K to produce clusters 8.8 ± 1.4 nm in diameter and 2.3 ± 0.5 nm in height; a 50 ML Ni film deposited at room temperature; and a 50 ML Ni film heated to 850 K. For the sake of brevity, the 3 and 8 ML Ni clusters will be referred to as small and large clusters, respectively. Our experiments show that the small Ni clusters and 50 ML film are more active for DMMP decomposition than the large clusters and 50 ML film annealed to 850 K. The decreased activity does not appear to be related to the size of the particles but is instead caused by changes that occur upon annealing the Ni surfaces. Because the removal of defects cannot completely explain the reduced activity of annealed Ni surfaces, we propose that the active sites on the Ni surfaces are blocked by diffusion of a TiO_x moiety from the support. The TiO_2(110) surface itself also decomposes DMMP, but the small Ni clusters and unannealed Ni film are both more active than titania. Lattice oxygen participates in the reaction of DMMP on the Ni clusters and films by oxidizing carbon to CO, which desorbs above 800 K.

Experimental Section

All experiments were performed in an ultrahigh vacuum chamber with a base pressure of 1 × 10^{-10} Torr built by Omicron Associates. The chamber is equipped with a variable temperature scanning tunneling microscope (Omicron, VT-STM25), X-ray photoelectron spectroscopy system (Omicron, EA125), low energy electron diffraction optics (Omicron, SPEC 3), mass spectrometer (Leybold Inficon, Transpector 2), sputter gun (Specs, IQE11), four pocket metal evaporator (Oxford Applied Research, EGCO4), and quartz crystal microbalance (Inficon). A more detailed description of this system is available elsewhere.[35,36]

A rutile TiO_2 single crystal (Commercial Crystals Inc.) cut along the (110) face and polished on one side was used for all experiments. The 1 cm × 1 cm × 0.1 cm crystal was mounted on a standard Omicron Ta sample plate directly above a 0.9 × 0.9 cm^2 hole, which was covered by 0.127 mm thick Ta foil. The sample temperature was monitored using a type K thermocouple spot welded onto the Ta plate near the edge of the crystal, and the crystal was fixed to the sample plate using spot-welded Ta straps along the edges. The sample heating stage was equipped with spring-loaded thermocouple pins that made contact with thermocouple buttons mounted on the bottom of the Ta plate, and the crystal could be heated to 1100 K by electron bombardment from a tungsten filament positioned directly behind the sample plate.[35,37] Our reported thermocouple measurement is believed to be ∼50 K higher than the true temperature of the crystal, based on a comparison with readings acquired at the same power settings for a thermocouple glued (Aremco 571) directly to the TiO_2 crystal.

The crystal was cleaned by repeated cycles of Ar^+ sputtering (30 min, 1 keV, 3 μA current to crystal) followed by annealing at 1000 K for 3 min. After several cleaning cycles, the crystal exhibited a blue color and a sharp (1 × 1), low energy electron diffraction (LEED) pattern. The cleanliness of the crystal was confirmed by X-ray photoelectron electron spectroscopy (XPS).

Ni was deposited onto the TiO_2 surface at room temperature using the Oxford Instruments electron beam evaporator. The Ni source consisted of a Ni rod (Alfa Aesar, 99.9995%) that was 23 mm long and 2 mm in diameter. Ni was evaporated at a rate of 0.5 ML/min and a background pressure of ∼6 × 10^{-10} Torr. The coverage of the deposited metal on the surface was calibrated by a quartz crystal microbalance as well as by scanning tunneling microscopy (STM) experiments.[35] One monolayer is defined with respect to the packing density of the Ni(111) surface (1.613 × 10^{15} atoms/cm^2). After each deposition, XPS and STM were used to characterize the surface cleanliness as well as the morphology of the deposited metal particles. All STM images were collected in constant current mode (∼+2 V, ∼0.2 nA) using electrochemically etched tungsten tips.[35,38]

DMMP was purchased from Aldrich (97% purity). NMR and GC/MS experiments were carried out to characterize the impurities in the DMMP sample, which was estimated to be 99% pure. A CH_3CH_2X compound is believed to account for

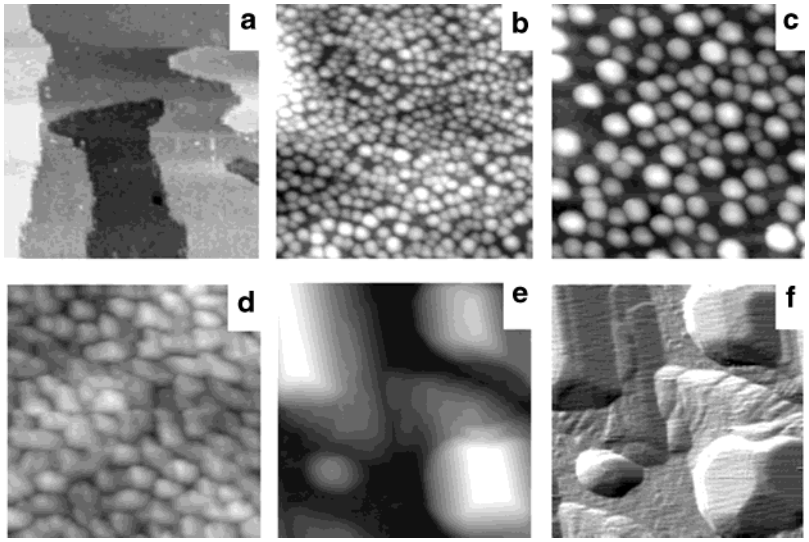

Figure 1. Scanning tunneling microscopy images of (a) TiO_2 (110); (b) the small Ni clusters (deposited at 295 K and flashed to 550 K); (c) the large Ni clusters (deposited at 295 K and annealed to 850 K); (d) the 50 ML Ni film deposited at 295 K; (e) the 50 ML Ni film deposited at 295 K and annealed to 850 K; and (f) the image in e differentiated to show the facets on the Ni islands. All images are 100 nm × 100 nm.

most of the 1% impurity, whereas CH_3Br accounted for less than 0.1%. Although CH_3Br is a common impurity in DMMP, it can be removed by freeze−pump−thaw cycles followed by pulling vacuum over the DMMP liquid while cooling in an ice−saltwater bath.[3] DMMP was introduced into chamber via a stainless steel directed dosing tube (11 mm diameter), which was positioned approximately 2 mm in front of the crystal. The crystal was exposed to a dose of 3×10^{-10} Torr for 3 min at room temperature, and X-ray photoelectron spectroscopy confirmed that this was a saturation exposure.

TPD experiments were carried out immediately after each DMMP dose using a linear temperature ramp of 2 K/s generated by a Eurotherm temperature controller (model 2408). The mass spectrometer was enclosed in a 5 cm diameter cylindrical stainless steel shroud capped by a movable flag with a 6 mm diameter hole cut in the center. The crystal was positioned directly in front of the hole and 5 mm from the end of the shroud during TPD experiments to minimize detected desorption from the sample holder. An in-house LabView program was used to collect up to 14 different masses in a single experiment; the thermocouple signal was also collected after passing it through an isolation amplifier (Analog Devices 5B40, 100× gain), which removed the 500 V bias applied to the crystal during electron bombardment heating. To establish that all relevant masses were being monitored, we conducted wide mass scan experiments on the TiO_2 surface as well as on the small Ni clusters and 50 ML Ni film; these TPD experiments collected all masses between 1 and 100 amu with lower temperature resolution.

All X-ray photoelectron spectra were acquired using a Mg Kα anode. Data for the C(1s) and P(2p) regions were collected with a 0.020 eV step and 0.2 s dwell time and averaged over three scans unless otherwise specified. For each data set, background P(2p) and C(1s) spectra for the clean TiO_2 or Ni surfaces were acquired before DMMP exposure. The background spectra of the surface contained no detectable phosphorus signal, but a small background carbon signal representing ∼5% of the carbon signal from a saturation dose of DMMP was observed; this contribution is believed to be from carbon on the Ta foil straps holding the crystal and is consistent with the small Ta signal observed when the uncollimated X-ray source irradiates the titania crystal and sample holder. All of the data shown in this paper represent spectra after the subtraction of a smoothed background spectrum. Peak fitting was carried out using Gaussian curves with a fwhm of 1.0−1.1 eV. Curve fits for the P(2p) doublet have the $2p_{3/2}$ and $2p_{1/2}$ peaks separated by 1.0 eV with a peak area ratio of 2:1, and the binding energy of the $2p_{3/2}$ peak is used to designate the position of the P(2p) doublet.

The Ni surface areas for the clusters and films were calculated from the STM images using a Matlab program. All images were plane flattened before the surface area analysis. The STM images were collected at a resolution of 512×512 pixels^2, with each pixel representing a point in 3D space with an *x*, *y*, and *z* coordinate. The projection of the STM image into the *xy* plane was divided into 511×511 squares, and each square was further divided into two triangles. The image surface area associated with each triangle was calculated using the *x*, *y*, and *z* coordinates of vertices, from which the lengths of the sides of the triangle were determined. The total area of the imaged surface was calculated by summing the surface areas associated with the 522 242 triangles. The fraction of surface area covered by Ni was found by subtracting the surface area corresponding to regions of exposed TiO_2 from the total surface area.

Results

STM Studies. In order to investigate particle size effects on DMMP decomposition, different sizes of Ni clusters and Ni films were prepared and imaged by STM (Figure 1). The average sizes of the Ni clusters were determined from STM line profiles, but because of tip convolution effects, the measured diameters may be larger than the actual ones.[39,40] Figure 1a shows a sputtered and annealed TiO_2 surface consisting of 30−70 nm wide terraces on which the bright atomic rows spaced by 0.65 nm are known to correspond to rows of Ti atoms.[41,42] Deposition of 3 ML of Ni onto this surface at room temperature followed by quickly heating to 550 K produced 3D clusters with a fairly uniform size distribution, as shown in Figure 1b. The average diameter and height of the clusters were approximately 5.0 ± 0.8 nm and 0.9 ± 0.2 nm, respectively, based on measurements from 20 clusters. Notably, the Ni clusters were initially heated to 550 K to remove any residual CO that was adsorbed during Ni deposition; however, the morphology and surface chemistry of the Ni clusters were identical before and after heating to 550 K. Large Ni clusters with an average

diameter of 8.8 ± 1.4 nm and a height of 2.3 ± 0.5 nm were prepared by the deposition of 8 ML of Ni at room temperature followed by heating the surface to 850 K with a linear temperature ramp of 2 K/s (Figure 1c). Although the small and large Ni clusters covered the majority of the TiO_2 surface, the clusters left 15 and 30% of the TiO_2 surface exposed, respectively. A Ni film that completely covered the titania surface was prepared by depositing 50 ML of Ni at room temperature (Figure 1d). Ni islands with an average width of 6.1 nm were observed, but the islands were irregularly shaped with no distinct facets. Heating this film to 850 K at 2 K/s produced large Ni islands roughly 30.0 nm wide and 13.2 nm high (Figure 1e). In addition to being much larger than the unannealed islands, these Ni islands had more regular shapes with facets that appear on the sides of the islands, as shown in the differentiated image (Figure 1f). Approximately 25% of the TiO_2 surface becomes exposed after annealing the 50 ML Ni film. During TPD of DMMP, the large Ni clusters as well as the annealed Ni film maintained their morphologies because both of the surfaces had already been heated to 850 K. However, heating to 850 K caused the small clusters to aggregate into larger clusters (average diameter 5.5 nm, height 2.0 nm), and the unannealed Ni film formed large domains similar to those in the annealed Ni film in Figure 1e.

TPD Studies. TPD experiments for DMMP reaction on the TiO_2 surface demonstrated that methyl (15 amu, corrected for DMMP and methane cracking) produces a sharp peak at 700 K (Figure 2a). Methane (16 amu) desorption is also observed in a broad feature with peaks at 435, 590, and 700 K, whereas H_2 (2 amu) desorption occurs over the same temperature range but has no distinct peaks. The 15 amu peak at 700 K is assigned to methyl radical desorption because its intensity is too high to be accounted for by methane and DMMP cracking and no higher masses are observed at this temperature. The desorption of molecular DMMP (79 amu) at 395 and 585 K was also detected. The 79 amu signal is used to represent DMMP desorption because the parent mass signal at 124 amu has much lower intensity and the cracking ratios for the 79, 94, and 109 amu signals relative to that at 124 amu were identical to that of DMMP itself. The cracking pattern for DMMP in our mass spectrometer was determined by leaking DMMP directly into the chamber, and a wide mass scan from 1 to 100 amu indicated that there were no masses detected other than those associated with the cracking of DMMP. Specifically, the desorption of a phosphorus-containing species (31 amu) and the desorption of water (18 amu) were not observed. The amount of methyl radical production was highly dependent on the extent of TiO_2 reduction, with the more reduced surfaces producing more methyl radicals. The methyl radical yield was smallest on a new TiO_2 crystal that had been subjected to only a few sputter−anneal cycles. Furthermore, reoxidizing the reduced TiO_2 surface by heating in 1×10^{-6} Torr of O_2 for an hour at 800 K also resulted in decreased methyl radical production.

DMMP reaction on the small 3 ML Ni clusters, which were deposited at room temperature and flashed to 550 K, produced CO (28 amu) and H_2 (2 amu) as the major products. CO desorption occurred in a large peak at 805 K and a smaller peak at 580 K (Figure 2b). The fact that the H_2 desorption peak at 580 K is larger than at 805 K suggests that the majority of DMMP decomposition occurs below 805 K. The main peak for DMMP desorption (79 amu) was at 400 K with a smaller shoulder at 630 K. Methane (16 amu) desorption resulted in a broad feature with distinct peaks at 470 and 585 K; note that the 16 amu peak at 805 K is due to the cracking of CO. There is no evidence for methyl radical desorption, given that the 15 and 16 amu signals had exactly the same peak shape with approximately the correct 15:16 amu ratio for methane.

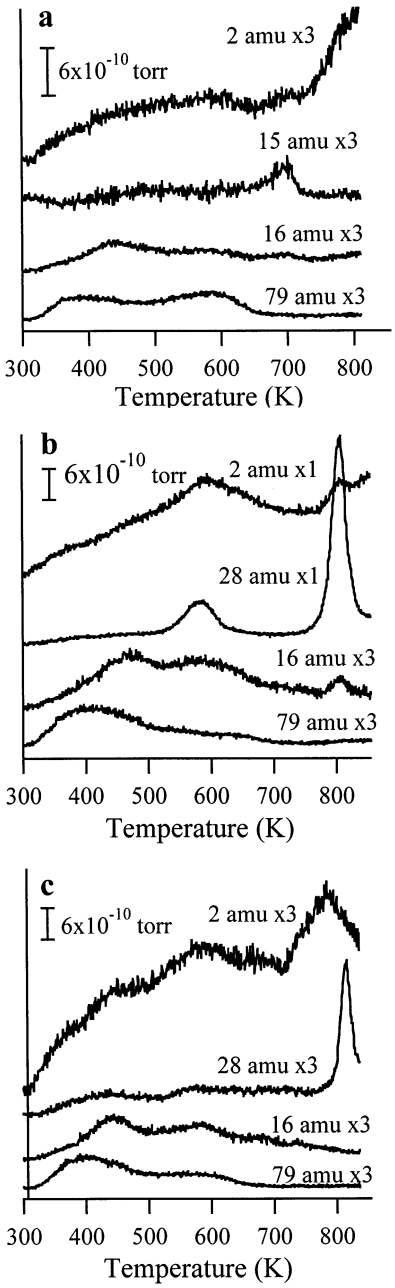

Figure 2. Temperature-programmed desorption data for a saturation dose of DMMP adsorbed at 295 K and heated with a linear ramp of 2 K/s on (a) TiO_2 (110); (b) the small Ni clusters; and (c) the large Ni clusters.

On the large Ni clusters (8 ML, annealed to 850 K), DMMP decomposition resulted in the same gaseous products, but the yields of CO and H_2 were much lower than on the small Ni clusters (Figure 2c). On the large Ni clusters, CO (28 amu) desorption occurred at 815 K, and the lower temperature desorption peak was not detected. The main intensity for the H_2 signal appeared above 785 K, suggesting that most of the C−H bond breaking occurs at high temperature. The desorption of DMMP (79 amu) and methane (16 amu) had roughly the same temperature profiles and intensities as those observed on the small Ni clusters except that the higher temperature DMMP peak was more distinct on the large Ni clusters. The intensity of the high temperature CO peak was very sensitive to the level

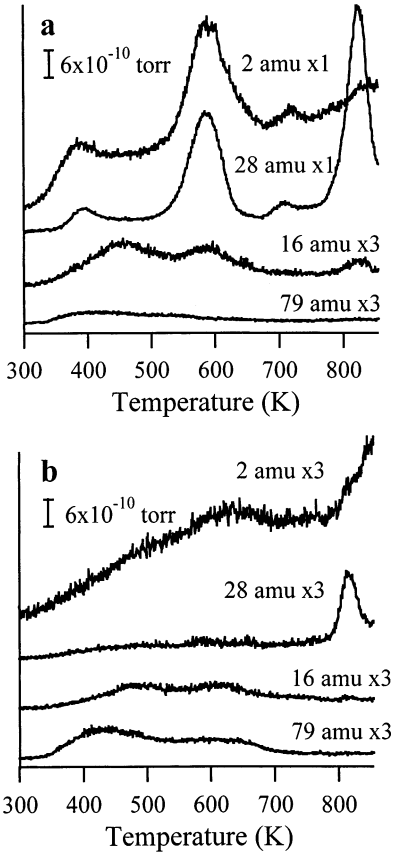

Figure 3. Temperature-programmed desorption data for a saturation dose of DMMP adsorbed at 295 K and heated with a linear ramp of 2 K/s on (a) the 50 ML Ni film deposited at 295 K and (b) the 50 ML Ni film deposited at 295 K and annealed to 850 K.

of reduction of the TiO_2 surface. On a more stoichiometric surface, the CO yield from the large clusters was 45% of that on the small clusters compared to 30% on the more reduced surface (Figure 2c).

DMMP reaction on a 50 ML Ni film deposited at room temperature resulted in large CO and H_2 desorption signals (Figure 3a). CO was produced in two large peaks at 585 and 825 K as well as two smaller peaks at 390 and 705 K. Although the H_2 and CO signals had similar profiles below 800 K, the dominant peak in the CO signal occurred at 825 K, which corresponded to the smallest of the H_2 peaks. This behavior is again consistent with the majority of DMMP decomposition occurring below ~700 K. For the 50 ML Ni film annealed to 850 K before exposure to DMMP, very little CO and H_2 were detected in the TPD experiment (Figure 3b), suggesting that annealing the Ni surfaces decreases the activity for DMMP decomposition. The desorption profiles and intensities for DMMP and methane desorption were similar on the large Ni clusters and annealed Ni film, but the integrated intensity for DMMP desorption was almost 50% lower on the unannealed film. The lack of DMMP desorption is consistent with the large CO and H_2 signals and indicates that most of the adsorbed DMMP decomposes on the unannealed film. Annealing the 50 ML Ni film to 550 K before DMMP desorption did not change the chemical activity of the film.

In order to understand the role of oxygen from the titania support on DMMP decomposition, the TiO_2 surface was reoxidized with $^{18}O_2$ before the deposition of the Ni clusters. The reoxidation treatment was carried out by exposing the TiO_2 surface to 1×10^{-7} Torr $^{18}O_2$ at 500 K for 30 min, followed by quickly heating to 800 K. For DMMP reactions on both the small and large Ni clusters, a high temperature peak around 805−815 K was observed for the 30 ($C^{18}O$) and 28 amu ($C^{16}O$) signals. The 30 amu signal accounted for 60−70% of the CO desorption, whereas the 28 amu signal accounted for 30−40%. On the small Ni clusters, the lower temperature 580 K CO desorption peak consisted only of the 28 amu signal and had no contribution from 30 amu. There was no evidence for incorporation of ^{18}O into DMMP itself (126 amu) on either the small or large Ni clusters. The production of $C^{18}O$ from DMMP decomposition on the unannealed 50 ML Ni film provides further evidence that a significant fraction of titania becomes exposed after heating the film to 850 K during the TPD experiment.

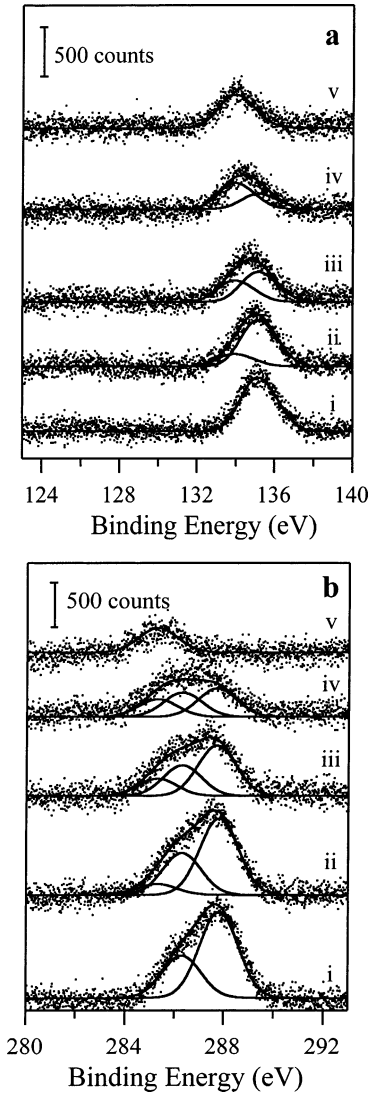

Figure 4. X-ray photoelectron spectra of the (a) P(2p) and (b) C(1s) regions for a saturation dose of DMMP on TiO_2(110) at (i) 295 K (no heating) and after heating to (ii) 400 K; (iii) 550 K; (iv) 650 K; and (v) 850 K. The temperature ramp used for heating was 2 K/s, and the step size during data acquisition was 0.01 eV.

XPS Studies. *DMMP Decomposition on TiO_2(110).* XPS data for DMMP on TiO_2(110) after heating to various temperatures demonstrates that multiple carbon and phosphorus species exist on the surface during the thermal decomposition of DMMP (Figure 4). TiO_2 was exposed to a saturation dose of DMMP at room temperature and then heated to 400, 550, 650, and 850 K with a linear temperature ramp of 2 K/s. The spectra shown in Figure 4 are nearly identical to those reported in an earlier study of DMMP decomposition on the more highly reduced TiO_2-

(110)-(1 × 2) surface.[36] Principal component analysis was used to establish that there were at least two linearly independent phosphorus-containing species and two linearly independent carbon-containing species on the TiO_2(110)-(1 × 2) surface between room temperature and 800 K, and the peak assignments described here are based on those for DMMP on TiO_2(110)-(1 × 2).[36] The main difference between DMMP reaction on the more stoichiometric (1 × 1) surface compared to that on the (1 × 2) surface is that the latter is slightly more reactive, and DMMP decomposition occurs even at room temperature. At room temperature, the P(2p) spectrum can be fit to a single peak at 134.9 eV, which has been assigned to phosphorus in molecular DMMP (Figure 4a). After the surface is heated to 400 K, a second P(2p) peak at 133.7 eV appears and is attributed to a PO_x species. As the surface is heated to higher temperatures, the 133.7 eV peak grows at the expense of the 134.9 eV peak, indicating DMMP decomposition, and only the 133.7 eV peak from PO_x is observed at 850 K. The phosphorus remaining on the TiO_2 surface could not be removed by further heating or by exposure to 1×10^{-6} Torr of O_2 gas at 850 K for 40 min. The C(1s) spectrum of DMMP at room temperature consists of two peaks at 287.8 and 286.3 eV (Figure 4b). These two peaks are assigned to the methoxy and methyl carbons in molecular DMMP, respectively, and have the expected peak area ratio of 2:1. At 400 K, a small peak at 285.3 eV appears in addition to the two higher binding energy peaks and is assigned to a decomposition species such as CH_x or atomic carbon.[36] Upon further heating, the 285.3 eV species accounts for a greater fraction of the total surface carbon, and the single peak at 850 K is attributed to atomic surface carbon, given that all of the gaseous decomposition products have desorbed at this temperature.

DMMP Decomposition on Ni Clusters and Films. As shown in Figure 5a, two peaks appear in the P(2p) spectrum for DMMP adsorbed on the small Ni clusters at room temperature, indicating that significant DMMP decomposition has already occurred upon adsorption, in contrast to behavior on the TiO_2 surface. The higher binding energy region can be fit with a peak at 134.5 eV, which is assigned to molecular DMMP based on a previous study of DMMP on Rh.[4] Notably the P(2p) binding energy for molecular DMMP on TiO_2 is slightly higher (134.9 eV) than that of DMMP on a transition metal surface. At 400 K, a new peak appears at ~129 eV and is assigned to atomic phosphorus adsorbed on Ni based on the 129 eV binding energy reported for atomic phosphorus on Rh.[4,43] The spectrum at 650 K can be fit with two peaks at 133.7 and 129.1 eV, with the former attributed to PO_x and the latter attributed to atomic phosphorus on Ni. After heating to 850 K, only atomic phosphorus on Ni is observed. The C(1s) spectra for DMMP on the small Ni clusters (Figure 5b) confirm that DMMP decomposes at room temperature, as demonstrated by the significant intensity at 285.3 eV and the fact that the methoxy and methyl peaks from molecular DMMP peaks do not have a 2:1 area ratio. The broadness of the C(1s) spectra even at room temperature reflects the presence of multiple carbon-containing species on the surface. Heating the surface above room temperature causes a change in the C(1s) peak shape as the lower binding energy peaks at ~283.5−284 eV appear. A comparison with the binding energy of atomic carbon on Ni(111)[44−46] suggests that atomic carbon is deposited on the Ni clusters. However, all of the carbon is removed from the surface after heating to 850 K.

A comparison of XPS data for DMMP adsorption at room temperature is shown in Figure 6 for the following surfaces: small Ni clusters, large Ni clusters, annealed Ni film, unannealed Ni film, and TiO_2. From the P(2p) data (Figure 6a), it is clear that the unannealed film is the most active for DMMP decomposition at room temperature because the 129 eV peak from atomic phosphorus on Ni is present. Furthermore, the small Ni clusters appear to be more active than all of the other surfaces with the exception of the unannealed film. The broadness of the P(2p) spectrum for the small Ni clusters suggests that there is more than one phosphorus species present, while the spectra on the titania surface can be fit to a single P(2p) doublet corresponding to molecular DMMP; the P(2p) spectra of the large Ni clusters and annealed Ni film have the main contribution from molecular DMMP. Based on the total integrated P(2p) signals, the relative saturation coverages of DMMP on these surfaces were estimated. The TiO_2 and small Ni clusters adsorb roughly the same amount of DMMP, whereas adsorption is 20% less on the large clusters and annealed film and 50% more on the unannealed film. Integrated intensities corresponding to the C(1s) region for DMMP adsorption at room temperature (Figure 6b) confirm the adsorption estimates from the P(2p) data. Again, the most DMMP decomposition is observed on the unannealed film, which has a C(1s) peak that is shifted to lower binding energy relative to that of the carbon species for molecular DMMP on TiO_2. This shift is also observed for DMMP on the small Ni clusters although it is less pronounced. For the annealed film and large Ni clusters, the C(1s) peak shape is more similar to that on the TiO_2 surface, where only molecular DMMP exists at room temperature.

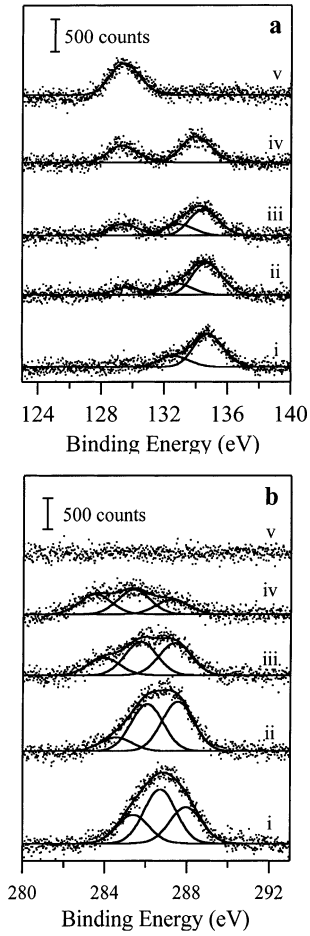

Figure 5. X-ray photoelectron spectra of the (a) P(2p) and (b) C(1s) regions for a saturation dose of DMMP on the small Ni clusters (3 ML) at (i) 295 K (no heating) and after heating to (ii) 400 K; (iii) 550 K; (iv) 650 K; and (v) 850 K. The temperature ramp used for heating was 2 K/s, and the step size during data acquisition was 0.02 eV.

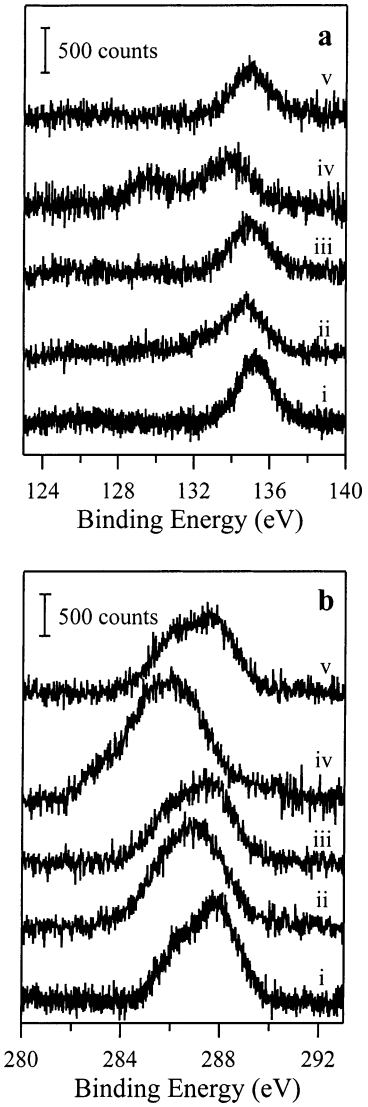

Figure 6. X-ray photoelectron spectra of the (a) P(2p) and (b) C(1s) regions after a saturation dose of DMMP at 295 K on (i) TiO_2 (110); (ii) the small Ni clusters; (iii) the large Ni clusters; (iv) the 50 ML Ni film deposited at 295 K; and (v) the 50 ML Ni film deposited at 295 K and annealed to 850 K. The step size during data acquisition was 0.02 eV on the Ni surfaces and 0.01 eV on TiO_2(110).

XPS spectra for DMMP adsorption followed by heating to 850 K are shown in Figure 7 for the four Ni surfaces and TiO_2. On all of the Ni surfaces, the main phosphorus species is atomic phosphorus on Ni with a binding energy of ~129 eV (Figure 7a). However, a major difference is that almost no phosphorus remains on the annealed film and large Ni clusters whereas the phosphorus signal is significant on the unannealed film and small Ni clusters. Given that no phosphorus-containing species desorb during heating, the amount of DMMP reaction on these surfaces can be estimated by dividing the integrated phosphorus signal after heating by the signal from DMMP adsorption at room temperature. In this manner, the percent reaction is calculated to be 85−90% on the small clusters and unannealed film compared with 55−60% on the large clusters, annealed film, and TiO_2 surface. The C(1s) data (Figure 7b) indicate that almost no carbon remains on the surface of the annealed film and large Ni clusters. Although small carbon signals were observed on the small Ni clusters and annealed film, only the unannealed Ni film had a carbon signal that was significantly above the baseline.

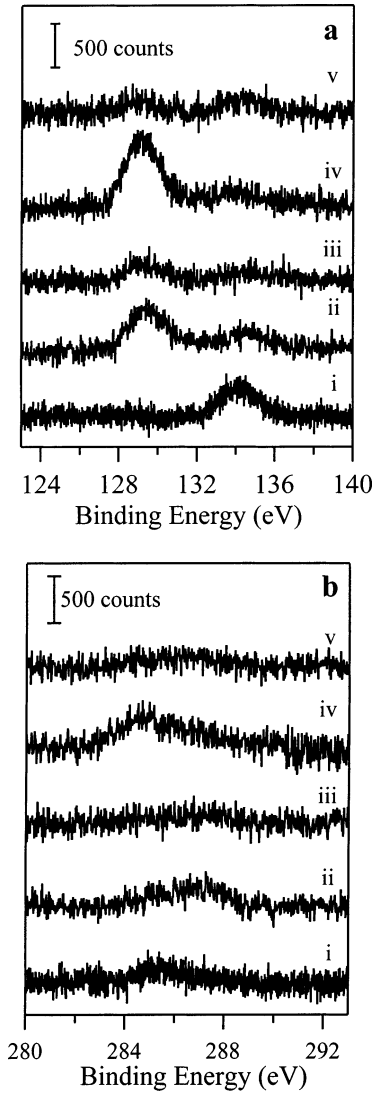

Figure 7. X-ray photoelectron spectra of the (a) P(2p) and (b) C(1s) regions after a saturation dose of DMMP followed by heating to 850 K at 2 K/s on (i) TiO_2 (110); (ii) the small Ni clusters; (iii) the large Ni clusters; (iv) the 50 ML Ni film deposited at 295 K; and (v) the 50 ML Ni film deposited at 295 K and annealed to 850 K. The step size during data acquisition was 0.02 eV on the Ni surfaces and 0.01 eV on TiO_2(110).

Discussion

Small Ni clusters (5.0 ± 0.8 nm diameter, 0.9 ± 0.2 nm height) supported on TiO_2(110) are found to be more active for DMMP decomposition than large Ni clusters (8.8 ± 1.4 nm diameter, 2.3 ± 0.5 nm height), which were deposited at room temperature and annealed to 850 K. More DMMP decomposition occurs at room temperature on the small clusters than on the larger ones. The greater activity of the small clusters is also reflected in the fact that nearly all of the adsorbed DMMP decomposes on the small clusters whereas only ~50% decomposes on the large clusters. DMMP decomposition and molecular desorption are competing processes on all of the Ni surfaces as well as the TiO_2 surface, and the amount of DMMP adsorption on the small and large clusters is comparable (within 20%). Notably, the TiO_2 surface itself has a DMMP saturation coverage similar to that of the small Ni clusters; therefore, DMMP adsorption is expected on exposed regions of the titania support as well as on the Ni clusters. The differently sized Ni clusters have different reactivities, but this behavior does not appear to be caused by cluster size effects. Instead, the loss of

chemical activity is attributed to the fact that the large clusters were annealed to 850 K whereas the small clusters were heated only to 550 K. Of the four Ni surfaces studied, the unannealed Ni film was the most active for DMMP decomposition, producing the greatest yields of CO and H_2 and leaving the most atomic phosphorus on the surface. DMMP reaction on the more ordered annealed film produced CO desorption only at 815 K, and the saturation coverage of DMMP at room temperature was approximately half of that on the unannealed film. Almost all of the DMMP adsorbed on the unannealed film is decomposed to produce atomic phosphorus, whereas only ~50% of the adsorbed DMMP is decomposed on the annealed film; this is consistent with the fact that much less DMMP is desorbed from the surface of the unannealed film.

Migration of a TiO_x moiety onto the Ni surface during annealing to 850 K could explain the lack of activity for the annealed Ni surfaces. Our XPS experiments indicate that the titania surface becomes reduced after annealing an 8 ML Ni film to 850 K. A shoulder in the Ti(2p) spectrum (data not shown) appears around 456−457 eV and is assigned to Ti^{3+}.[47] It is not surprising that titania is reduced by the Ni clusters, given that previous photoelectron spectroscopy experiments[28,29] as well as theoretical studies[48] have shown that there are electronic interactions between Ni clusters and the titania support. The initial deposition of the 8 ML Ni film does not result in a change in the Ti(2p) peak shape, indicating that titania is not reduced by the deposition of Ni at room temperature. Moreover, annealing this Ni film to 600 K does not change the Ti(2p) peak shape. A slight shoulder around 456−457 eV first appears after heating to 700 K, and the intensity of the shoulder continues to increase after annealing to 800 and 850 K. Similarly, there is little change in the Ni(2p) intensity after annealing to 700 K although there is an ~0.1 eV shift to higher binding energy. Heating to 850 K causes a 20% drop in integrated peak intensity as well as a +0.25 eV shift in binding energy compared to the Ni($2p_{3/2}$) position at room temperature. The loss of signal intensity is partially due to the agglomeration of the Ni film, which forms large Ni clusters at 850 K. The slight shift in the Ni($2p_{3/2}$) position to higher binding energy may indicate that the Ni clusters have become oxidized, but shifts to higher binding energies have also been observed for supported metal clusters and films with increasing coverage and size.[15,49] It is possible that a reduced TiO_x moiety diffuses onto the Ni clusters during annealing since heating the deposited Ni to high temperatures is necessary to observe reduction of the titania support.

Investigations of Ni clusters supported on titania powders have reported that Ni clusters become encapsulated with TiO_x after heating to 773 K in a hydrogen atmosphere.[50−54] When Ni clusters on titania are reduced at high temperature, the capacity for CO and H_2 adsorption on these surfaces is diminished,[55−58] and this behavior has been described as a strong metal support interaction (SMSI). Transmission electron microscopy (TEM) studies have shown that titania-supported Ni clusters become covered with a species that was identified as Ti_4O_7 after reduction in H_2 at 1000 K.[59] The growth of TiO_x films on polycrystalline Ni surfaces decreases the capacity for CO and H_2 adsorption in a manner similar to the SMSI behavior.[58] In ultrahigh vacuum, other transition metal clusters such as Pt,[60−64] Rh,[65−67] and Pd[68−70] deposited on TiO_2 are known to become encapsulated by TiO_x upon heating.[33,71] Studies of smaller Ni clusters (2−15 atoms) on TiO_2(110) by Anderson and co-workers have demonstrated that the Ni clusters become less active for CO adsorption after annealing to 600 K in ultrahigh vacuum.[72] Low energy ion scattering (LEIS) experiments showed that the Ni signal decreased upon annealing but did not disappear completely. Although the sintering of the Ni clusters could explain some of these effects, partial encapsulation of the Ni clusters could not be completely ruled out. Clusters consisting of only a few atoms are more likely to become encapsulated compared to the larger clusters and films investigated in this work, but Anderson and co-workers did not heat the supported Ni clusters above 600 K. Our studies have shown that heating the Ni clusters or the 50 ML film to 550 K also does not change the reactivity of the Ni surface whereas heating to 850 K shuts down chemical activity.

Another possible explanation for the reduced surface activity is that annealing causes a loss of high coordination defect sites, which are presumably the active sites for DMMP decomposition. Freund and co-workers' investigations of alumina-supported Pd particles report that the particle surfaces are more defective than Pd(111) due to an increased number of step and edge defects.[11,73−76] Møller and Wu's infrared studies of CO adsorption on Ni films on TiO_2(110) show that CO adsorption on defect sites at the edges of Ni islands results in a ν(CO) frequency that is lower than that observed on (111) surfaces.[77] Therefore, it is reasonable to expect that the small Ni clusters and unannealed Ni film deposited at room temperature are also more defective, with a greater number of high coordination sites than either single crystal Ni surfaces or Ni surfaces that have been annealed to 850 K. The paraboloid shapes of the small Ni clusters as imaged by STM do not show any evidence of ordered structures. Although it is possible that the STM tip is not capable of resolving finer detail on this size scale, TEM studies by Tanner et al. also report that at low Ni coverages the Ni clusters initially grow as small crystalline domes without any preferential orientation with respect to the titania surface.[24] The large clusters annealed to 850 K appear to have paraboloid shapes, but there is some evidence from the line profiles and STM images that facets are beginning to form in the larger clusters. The Ni film annealed to 850 K consists of large Ni islands with regular shapes as well as facets on the sides in contrast to the unannealed film, which is composed of irregularly shaped islands that have randomly grown together. The islands in the annealed Ni film are similar to the "hut-clusters" reported by Tanner et al. for annealed Ni islands on TiO_2;[24] the tops of the Ni islands have rooflike shapes, and the sides of the islands are inclined 35° from the plane of the titania surface. Tanner et al. concluded that the surfaces of the annealed Ni islands consist mainly of {111} and {100} facets.[24]

Although the unannealed clusters and films may be more defective than the annealed Ni surfaces, the reduced number of high coordination sites cannot completely explain the lack of reactivity for the annealed surfaces. Previous studies of DMMP decomposition on the Ni(111) surface show that CO and H_2 are produced with significant yields, and both the low and high temperature CO desorption peaks were observed.[6] Because the annealed Ni clusters and film must contain more high coordination sites than the Ni(111) surface, the lack of CO production on the annealed surfaces cannot be solely attributed to the removal of these defects on the Ni surfaces after heating. However, defects very likely play a role in the enhanced DMMP decomposition on the unannealed Ni surfaces; the 50 ML Ni film has only ~25% more surface area than the small clusters, but the unannealed film produces twice as much CO from DMMP decomposition. The fact that four CO desorption peaks are observed for DMMP decomposition on the unannealed film suggests that there is more than one type of active site on this

TABLE 1: Comparison of Surface Areas, DMMP Adsorption, and CO Yields from DMMP Decomposition and CO Desorption for the Five Surfaces Studied[a]

surface	small Ni clusters (3 ML)	large Ni clusters (8 ML, annealed to 850 K)	50 ML Ni film (unannealed)	50 ML Ni film (annealed to 850 K)	TiO_2(110)
Ni surface area	1.00	0.96	1.25	0.92	0
% uncovered TiO_2	15	30	0	25	100
total surface area (TiO_2 + Ni)	1.00	1.09	1.08	1.01	0.85
DMMP adsorption	1.00	0.80	1.50	0.80	0.96
CO yield from DMMP decomposition	1.00	0.27	2.02	0.08	0
CO desorption yield	1.00	0.30	3.00	0.30	0

[a] All values are normalized to those of the small Ni clusters. The value for DMMP adsorption was determined from the P(2p) area for DMMP adsorbed at room temperature.

surface. Only two CO desorption peaks are observed for DMMP decomposition on the small Ni clusters, with the 580 K peak assigned to molecular desorption and the 805 K peak assigned to the recombination of atomic carbon and oxygen. On the unannealed film, most of the CO intensity is also in the 580 and 820 K peaks, but smaller desorption features at 400 and 710 K appear. DMMP decomposition on the annealed film and clusters resulted in only one CO desorption peak around 815 K.

Since the desorption of CO from Ni surfaces has been well studied in the literature, CO desorption experiments on the four Ni surfaces were carried out in order to better understand the adsorption sites. To compare the total CO desorption yields on the four different Ni surfaces, these values were normalized against CO desorption on the small Ni clusters (Table 1). CO desorption on the unannealed Ni film was 3 times higher than on the small clusters, whereas desorption from the annealed film and large clusters was only 30% of that on the small clusters. Although the surfaces of the annealed clusters and films should be less defective compared to their unannealed counterparts, the lack of surface defects cannot explain the decreased CO adsorption. Based on experiments reported in the literature, CO adsorbs strongly on closed-packed Ni surfaces such as (111),[78−80] (110),[81] and (100).[82−85] In many of these experiments reported in the literature, CO was adsorbed at 100 K, whereas our experiments conducted on the Ni clusters and films involved adsorption at room temperature; however, the adsorption of CO on single crystal surfaces at room temperature is known to be very similar to adsorption at low temperature,[86] and the sticking coefficient of CO on Ni(111) at room temperature is near unity.[87] CO should therefore adsorb equally strongly on the annealed Ni clusters and film, which have surface structures similar to the close-packed faces of Ni. The lack of CO adsorption on the annealed Ni surfaces is further evidence that active sites become blocked by TiO_x or oxygen migrating from the titania support.

The decreased activity of the annealed Ni surfaces is not due to a loss of Ni surface area after annealing. As shown in Table 1, the small and large clusters as well as the annealed Ni film have approximately the same Ni surface area despite the fact that the product yields of CO and H_2 on the small clusters are substantially higher. Estimates of the surface area of the Ni clusters from the cluster densities and average sizes of the clusters, which were assumed to have a paraboloid shape, are also consistent with the small and large clusters having the same surface areas. It is possible that the measured cluster sizes are overestimated due to tip convolution effects. Because tip convolution effects are more pronounced in the case of the small clusters, the calculated surface area of the small clusters would be overestimated compared to that of the large clusters and annealed film. Therefore, the lower activity of the annealed Ni surfaces cannot be due to reduced Ni surface area, which should be at least as great as the surface area of the small clusters. Furthermore, the small clusters actually sinter and lose surface area during the thermal decomposition of DMMP, whereas the annealed clusters and film maintain the same surface area and morphology. In Table 1, it is assumed that the area between the Ni clusters corresponds to the uncovered TiO_2 surface; it is still possible that these regions contain very small Ni clusters that are difficult to image in the presence of features with much larger aspect ratios even though there is no evidence for such islands in the STM images. However, the purpose of this surface area analysis is only to establish that the annealed clusters still have surface area comparable to that of the unannealed clusters; therefore, ignoring the surface area of small Ni islands does not change the overall conclusion.

The TiO_2(110) surface itself also decomposes DMMP, but titania is much less active than the small Ni clusters and produces significantly less H_2. Instead of decomposing DMMP into CO, as observed on the Ni surfaces, methane and methyl radicals are the main carbon-containing products that desorb from TiO_2. On the Ni surfaces, approximately the same amount of methane is produced from DMMP decomposition as on TiO_2. However, methyl radical desorption is not observed from the Ni surfaces, presumably because Ni is more active for C−H bond breaking compared to TiO_2, and methyl intermediates would therefore be more likely to decompose to atomic carbon on Ni. The extent of methyl radical production is related to the level of reduction of the TiO_2 surface, with the more reduced surfaces producing the greatest methyl radical yield. Other studies of chemical reactions on rutile TiO_2(110) have demonstrated that surfaces with a greater number of oxygen vacancies, which can be created either by annealing or by electron bombardment, are more chemically active.[88] For example, molecules such as O_2,[89] CO,[90] and formic acid[91] are more easily adsorbed on TiO_2 surfaces with oxygen vacancies. Oxygen vacancies also played an important role in the reactions of N_2O,[92,93] NO_2,[94] H_2O,[95] C_2H_2,[93] and methanol[96] on TiO_2. Anatase TiO_2 surfaces that were sputtered to create more Ti^{3+} sites decomposed formic acid, whereas the fully oxidized surfaces did not.[97]

The amount of DMMP that adsorbs or reacts at room temperature on the Ni and TiO_2 surfaces can be discussed in terms of relative surface areas. The combined Ni and titania surface areas shown in Table 1 indicate that the Ni clusters and films have approximately the same total surface area, and the surface area of TiO_2 is ∼15% lower. The TiO_2 surface and the small Ni clusters adsorb roughly the same amount of DMMP. However, the annealed Ni clusters and film adsorb ∼20% less, providing further evidence for the lack of active sites on the annealed Ni surfaces. The unannealed Ni film adsorbs ∼50% more DMMP even though the total surface area is approximately

the same, and this result suggests that the increased activity of the unannealed film is due to a greater number of active sites.

Although the small Ni clusters and TiO_2(110) adsorb roughly the same amount of DMMP, decomposition occurs at room temperature on the Ni clusters, whereas only molecular DMMP is observed on the TiO_2 surface. Furthermore, nearly all of the adsorbed DMMP reacts on the small Ni clusters after heating to 850 K, but only ~50% of the DMMP decomposes on TiO_2. Phosphorus remaining on the TiO_2 surface after DMMP decomposition is believed to contain intact P−O, based on the 133.7 eV P(2p) peak in the x-ray photoelectron spectrum.[36] Either the P−O bonds in DMMP are not broken on TiO_2 or atomic phosphorus binds to lattice oxygen on titania. In contrast, phosphorus remaining on the Ni clusters is assigned to atomic phosphorus on a metal surface based on the 129 eV binding energy. Although the sintering of the small Ni clusters leaves the TiO_2 surface exposed after heating to 850 K, the absence of the 133.7 eV phosphorus species indicates that phosphorus is bound to Ni rather than TiO_2. This suggests that DMMP decomposition occurs preferentially on the Ni surface even when a significant fraction of the TiO_2 surface is exposed. Moreover, methyl radical production from the reaction on TiO_2 is not observed when the Ni clusters do not cover all of the TiO_2 surface.

Despite the fact that the Ni clusters shut down the reactivity of the TiO_2 support itself, the TiO_2 surface still plays an important role in the production of CO from DMMP decomposition on the Ni surfaces. When TiO_2 is reoxidized with $^{18}O_2$ before Ni deposition, DMMP decomposition on these surfaces produced $C^{18}O$ as well as $C^{16}O$ at 805−820 K; for the small Ni clusters, only $C^{16}O$ is produced at 580 K. These experiments confirm that the C−O bond in DMMP is broken, and the high temperature CO desorption involves the oxidation of atomic carbon by oxygen from the titania lattice. $C^{16}O$ desorption at 805−820 K may be attributed to atomic oxygen from the decomposition of DMMP, but this $C^{16}O$ desorption could also be due to oxygen from titania because the majority of the oxygen in the TiO_2 lattice is still ^{16}O. The absence of $C^{18}O$ desorption at 580 K on the small Ni clusters indicates that at these lower temperatures either C−O bond scission in DMMP does not occur or oxygen from TiO_2 oxygen does not migrate onto Ni. The small or nonexistent carbon signals on the Ni surfaces after heating to 850 K are consistent with the fact that most of the deposited carbon is oxidized to CO. The decomposition of DMMP on the annealed 50 ML Ni films also results in the production of $C^{18}O$ at 815 K; since the annealed film consists of large 3D islands with an average height of ~13 nm covering ~75% of the surface, the oxidation of carbon is expected to occur at the edges of the Ni−TiO_2 interface unless lattice oxygen is capable of diffusing over relatively long distances on the Ni islands. Oxygen migration onto the Ni surface is assumed rather than carbon migration onto TiO_2 because atomic carbon cannot be oxidized to CO on TiO_2 but can be oxidized on Ni surfaces. The higher desorption temperature of recombinant CO on the Ni clusters and films compared to that on Ni(111) (805−820 K vs 600 K)[6] can be understood in terms of the higher temperatures required for the diffusion of lattice oxygen. Other studies have shown evidence for interactions between surface intermediates and oxygen from the metal oxide surface. For example, carbon deposited from CO dissociation on TiO_2-supported Rh clusters is oxidized by lattice oxygen from titania between 800 and 1300 K to produce CO.[98] In the combustion of methane over Pd particles on alumina and zirconia, oxygen from the support is incorporated into the CO and CO_2 oxidation products.[99] O_2 is also known to dissociate on Pd clusters on TiO_2 and provide oxygen atoms that spill over onto the titania support.[68] Furthermore, the decomposition of formic acid on TiO_2(110) produces oxygen atoms that are incorporated into the titania surface.[100]

In terms of the catalytic decomposition of DMMP, it is known that phosphorus-containing species left on the surface will passivate the surface toward further DMMP reaction. Therefore, it is useful to understand the types of phosphorus remaining on the surface after thermal decomposition of DMMP to 850 K. Unfortunately, phosphorus bound on lattice oxygen ($P-O_{lattice}$) and a phosphorus-containing species with intact P−O bonds (PO_x) cannot be distinguished based on the P(2p) binding energies because both should occur around 133.7 eV. However, atomic phosphorus on Ni (P−Ni) can be distinguished based on its lower binding energy of 129 eV. On the TiO_2 surface, only the 133.7 eV peak is observed after heating to 850 K, indicating that this surface does not break all P−O bonds or that atomic phosphorus is bound to lattice oxygen. On both the unannealed Ni film and small Ni clusters, almost all of the surface phosphorus exists as P−Ni, indicating that most P−O bonds are broken on these surfaces. On the annealed Ni films and large clusters, the 133.7 and 129 eV peaks are of comparable intensity; the total phosphorus signal intensity is relatively small due to decreased total reaction on the annealed Ni surfaces. Because the 50 ML Ni films completely cover the TiO_2 surface, it is most likely that the 133.7 eV peak is due to PO_x rather than $P-O_{lattice}$, suggesting that not all P−O bonds are broken, which is consistent with the lower overall reactivity of the annealed Ni surfaces.

The TiO_2-supported Ni clusters are not ideal materials for the catalytic composition of DMMP. Ni clusters and film deposited at room temperature have high activity for DMMP decomposition, but atomic carbon and phosphorus are deposited on the surface, which is passivated toward further reaction. Although carbon can be removed from the surface as CO above 805−815 K, heating to these temperatures will also cause the Ni surfaces to lose most of their activity. Furthermore, phosphorus cannot be easily removed from Ni surfaces even by treatment in oxygen at high temperature.[6] In any case, it is important to understand that the titania substrate is an active participant in the decomposition of DMMP, either by providing oxygen for the removal of surface carbon as CO or by the possible migration of TiO_x onto the Ni surfaces.

Conclusions

The addition of Ni to TiO_2(110) changes the reaction pathways for DMMP surface decomposition although the decomposition pathways are not affected by the amount of Ni deposited or the extent of annealing. All of the supported Ni surfaces produced CO and H_2 as the major gaseous products, whereas the TiO_2 surface produced methyl radicals, methane, and H_2 as the main decomposition products. However, the activity for DMMP decomposition is greatly decreased by annealing the Ni surfaces. This reduction in activity cannot be completely explained by a loss in Ni surface area or a loss of high coordination defect sites during annealing. Therefore, the diffusion of a TiO_x species onto the Ni surfaces is proposed to contribute to both the lack of DMMP decomposition and the lack of CO adsorption on the annealed surfaces. Small Ni clusters on TiO_2(110) were more active for DMMP decomposition than large annealed Ni clusters, but this difference in chemical activity is not attributed to a cluster size effect. The Ni clusters and films supported on TiO_2 cannot be considered

to be surfaces for catalytic DMMP decomposition because the reaction leaves carbon and phosphorus on the surface. Although carbon on the Ni surfaces is oxidized to CO above 800 K by oxygen from the TiO_2 lattice, phosphorus cannot be removed.

Acknowledgment. We gratefully acknowledge financial support from the U.S. Army Research Office under a Young Investigator Award (DAAD19-00-1-0557); the Department of Energy, Office of Basic Energy Sciences under a DOE/EPSCOR grant (DE-FG02-01ER45892), and the National Science Foundation under a CAREER Award (CHE 0133926). We also thank M. L. Myrick (University of South Carolina) for his help in writing the Matlab program for calculating surface areas.

References and Notes

(1) Yang, Y.-C.; Baker, J. A.; Ward, J. R. *Chem. Rev.* **1992**, *92*, 1729.
(2) Ekerdt, J. G.; Klabunde, K. J.; Shapley, J. R.; White, J. M.; Yates, J. T. *J. Phys. Chem.* **1988**, *92*, 6182.
(3) Henderson, M. A.; White, J. M. *J. Am. Chem. Soc.* **1988**, *110*, 6939.
(4) Hegde, R. I.; Greenlief, C. M.; White, J. M. *J. Phys. Chem.* **1985**, *89*, 2886.
(5) Smentkowski, V. S.; Hagans, P.; Yates, J. T. *J. Phys. Chem.* **1988**, *92*, 6351.
(6) Guo, X.; Yoshinobu, J.; Yates, J. T. *J. Phys. Chem.* **1990**, *94*, 6839.
(7) Okumura, M.; Kitagawa, Y.; Haruta, M.; Yamaguchi, K. *Chem. Phys. Lett.* **2001**, *346*, 163.
(8) Haruta, M.; Date, M. *Appl. Catal., A* **2001**, *222*, 427.
(9) Haruta, M. *CATTECH* **2002**, *6*, 102.
(10) Sakurai, H.; Tsubota, S.; Haruta, M. *Appl. Catal., A* **1993**, *102*, 125.
(11) Cunningham, D. A. H.; Vogel, W.; Sanchez, R. M. T.; Tanaka, K.; Haruta, M. *J. Catal.* **1999**, *183*, 24.
(12) Iizuka, Y.; Tode, T.; Takao, T.; Yatsu, K.; Takeuchi, T.; Tsubota, S.; Haruta, M. *J. Catal.* **1999**, *187*, 50.
(13) Hayashi, T.; Tanaka, K.; Haruta, M. *J. Catal.* **1998**, *178*, 566.
(14) Sakurai, H.; Ueda, A.; Kobayashi, T.; Haruta, M. *Chem. Commun.* **1997**, 271.
(15) Henry, C. R. *Surf. Sci. Rep.* **1998**, *31*, 231.
(16) Santra, A. K.; Goodman, D. W. *J. Phys.: Condens. Matter* **2003**, *15*, 31.
(17) Xu, X.; Goodman, D. W. *Catal. Lett.* **1994**, *24*, 31.
(18) Keane, M. A.; Park, C.; Menini, C. *Catal. Lett.* **2003**, *88*, 89.
(19) Pina, G.; Louis, C.; Keane, M. A. *Phys. Chem. Chem. Phys.* **2003**, *5*, 1924.
(20) Guczi, L.; Peto, G.; Beck, A.; Frey, K.; Geszti, O.; Molnar, G.; Daroczi, C. *J. Am. Chem. Soc.* **2003**, *125*, 4332.
(21) Bae, J. W.; Kim, I. G.; Lee, J. S.; Lee, K. H.; Jang, E. J. *Appl. Catal., A.* **2003**, *240*, 129.
(22) Zemichael, F. W.; Palermo, A.; Tikhov, M. S.; Lambert, R. M. *Catal. Lett.* **2002**, *80*, 93.
(23) Zhou, J.; Kang, Y. C.; Chen, D. A. *Surf. Sci.* **2003**, *537*, L429.
(24) Tanner, R. E.; Goldfarb, I.; Castell, M. R.; Briggs, G. A. D. *Surf. Sci.* **2001**, *486*, 167.
(25) Somorjai, G. A. *Chemistry in Two Dimensions: Surfaces*; Cornell University Press: Ithaca, NY, 1981.
(26) Somorjai, G. A. *Introduction to Surface Chemistry and Catalysis*; John Wiley and Sons: New York, 1994.
(27) Mullins, D. R. *J. Phys. Chem. B* **1997**, *101*, 1014.
(28) Kao, C. C.; Tsai, S. C.; Bahl, M. K.; Chung, Y. W.; Lo, W. J. *Surf. Sci.* **1980**, *95*, 1.
(29) Onishi, H.; Aruga, T.; Egawa, C.; Iwasawa, Y. *Surf. Sci.* **1990**, *233*, 261.
(30) Diebold, U.; Tao, H. S.; Shinn, N. D.; Madey, T. E. *Phys. Rev. B* **1994**, *50*, 14474.
(31) Pan, J.-M.; Madey, T. E. *J. Vac. Sci. Technol., A* **1993**, *11*, 1667.
(32) Pan, J. M.; Diebold, U.; Zhang, L. Z.; Madey, T. E. *Surf. Sci.* **1993**, *295*, 411.
(33) Diebold, U.; Pan, J. M.; Madey, T. E. *Surf. Sci.* **1995**, *333*, 845.
(34) Diebold, U. *Surf. Sci. Rep.* **2003**, *48*, 53.
(35) Zhou, J.; Chen, D. A. *Surf. Sci.* **2003**, *527*, 183.
(36) Zhou, J.; Varazo, K.; Reddic, J. E.; Myrick, M. L.; Chen, D. A. *Anal. Chim. Acta* **2003**, *496*, 289.
(37) Illingworth, A.; Zhou, J.; Ozturk, O.; Chen, D. A. *J. Vac. Sci. Technol., B.*, in press, 2004.
(38) Reddic, J. E.; Zhou, J.; Chen, D. A. *Surf. Sci.* **2001**, *494*, L767.
(39) Chen, D. A.; Bartelt, M. C.; McCarty, K. F.; Hwang, R. Q. *Surf. Sci.* **2000**, *450*, 78.
(40) Stempel, S.; Bäumer, M.; Freund, H. J. *Surf. Sci.* **1998**, *404*, 424.
(41) Diebold, U.; Anderson, J. F.; Ng, K. O.; Vanderbilt, D. *Phys. Rev. Lett.* **1996**, *77*, 1322.
(42) Diebold, U.; Lehman, J.; Mahmoud, T.; Kuhn, M.; Leonardelli, G.; Hebenstreit, W.; Schmid, M.; Varga, P. *Surf. Sci.* **1998**, *411*, 135.
(43) Greenlief, C. M.; Hedge, R. I.; White, J. M. *J. Phys. Chem.* **1985**, *89*, 5681.
(44) Rufael, T. S.; Huntley, D. R.; Mullins, D. R.; Gland, J. L. *J. Phys. Chem.* **1995**, *99*, 11472.
(45) Huntley, D. R.; Jordan, S. L.; Grimm, F. A. *J. Phys. Chem.* **1992**, *96*, 1409.
(46) Dickens, K. A.; Stair, P. C. *Langmuir* **1998**, *14*, 1444.
(47) Pan, J. M.; Maschhoff, B. L.; Diebold, U.; Madey, T. E. *J. Vac. Sci. Technol., A* **1992**, *10*, 2470.
(48) Cao, P. L.; Ellis, D. E.; Dravid, V. P. *J. Mater. Res.* **1999**, *14*, 3684.
(49) Chusuei, C. C.; Lai, X.; Luo, K.; Goodman, D. W. *Top. Catal.* **2001**, *14*, 71.
(50) Bradford, M. C. J.; Vannice, M. A. *Appl. Catal., A* **1996**, *142*, 73.
(51) Tauster, S. J. *Acc. Chem. Res.* **1987**, *20*, 389.
(52) Smith, J. S.; Thrower, P. A.; Vannice, M. A. *J. Catal.* **1981**, *68*, 270.
(53) Takatani, S.; Chung, Y. W. *Appl. Surf. Sci.* **1984**, *19*, 341.
(54) Raupp, G. B.; Dumesic, J. A. *J. Catal.* **1986**, *97*, 85.
(55) Osaki, T. *J. Chem. Soc., Faraday Trans.* **1997**, *93*, 643.
(56) vandeLoosdrecht, J.; vanderKraan, A. M.; vanDillen, A. J.; Geus, J. W. *J. Catal.* **1997**, *170*, 217.
(57) Burch, R.; Flambard, A. R. *J. Catal.* **1982**, *78*, 389.
(58) Raupp, G. B.; Dumesic, J. A. *J. Phys. Chem.* **1984**, *88*, 660.
(59) Dumesic, J. A.; Stevenson, S. A.; Sherwood, R. D.; Baker, R. T. K. *J. Catal.* **1986**, *99*, 79.
(60) Dulub, O.; Hebenstreit, W.; Diebold, U. *Phys. Rev. Lett.* **2000**, *84*, 3646.
(61) Jennison, D. R.; Dulub, O.; Hebenstreit, W.; Diebold, U. *Surf. Sci.* **2001**, *492*, L677.
(62) Pesty, F.; Steinrück, H.-P.; Madey, T. E. *Surf. Sci.* **1995**, *339*, 83.
(63) Berko, A.; Szoko, J.; Solymosi, F. *Surf. Sci.* **2003**, *532*, 390.
(64) Szoko, J.; Berko, A. *Vacuum* **2003**, *71*, 193.
(65) Berkó, A.; Ulrych, I.; Prince, K. C. *J. Phys. Chem. B* **1998**, *102*, 3379.
(66) Berkó, A.; Solymosi, F. *Surf. Sci.* **1998**, *400*, 281.
(67) Berkó, A.; Mensesi, G.; Solymosi, F. *Surf. Sci.* **1997**, *372*, 202.
(68) Bowker, M.; Smith, R. D.; Bennett, R. A. *Surf. Sci.* **2001**, *478*, L309.
(69) Bennett, R. A.; Stone, P.; Bowker, M. *Faraday Discuss.* **2000**, *114*, 267.
(70) Suzuki, T.; Souda, R. *Surf. Sci.* **2000**, *448*, 33.
(71) Campbell, C. T. *Surf. Sci. Rep.* **1997**, *27*, 1.
(72) Aizawa, M.; Lee, S.; Anderson, S. L. *J. Chem. Phys.* **2002**, *117*, 5001.
(73) Yudanov, I. V.; Sahnoun, R.; Neyman, K. M.; Rosch, N.; Hoffmann, J.; Schauermann, S.; Johanek, V.; Unterhalt, H.; Rupprechter, G.; Libuda, J.; Freund, H. J. *J. Phys. Chem. B* **2003**, *107*, 255.
(74) Rupprechter, G.; Unterhalt, H.; Morkel, M.; Galletto, P.; Hu, L. J.; Freund, H. J. *Surf. Sci.* **2002**, *502*, 109.
(75) Schauermann, S.; Hoffmann, J.; Johanek, V.; Hartmann, J.; Libuda, J.; Freund, H. J. *Catal. Lett.* **2002**, *84*, 209.
(76) Stroscio, J. A.; Pierce, D. T. *Phys. Rev. B* **1994**, *49*, 8522.
(77) Wu, M. C.; Møller, P. J. *Surf. Sci.* **1991**, *250*, 179.
(78) Xu, Z.; Surnev, L.; Uram, K. J.; Yates, J. T. *Surf. Sci.* **1993**, *292*, 235.
(79) Miller, J. B.; Siddiqui, H. R.; Gates, S. M.; Russell, J. N.; Yates, J. T.; Tully, J. C.; Cardillo, M. J. *J. Chem. Phys.* **1987**, *87*, 6725.
(80) Trenary, M.; Uram, K. J.; Yates, J. T. *Surf. Sci.* **1985**, *157*, 512.
(81) Feigerle, C. S.; Overbury, S. H.; Huntley, D. R. *J. Chem. Phys.* **1991**, *94*, 6264.
(82) Muscat, A. J.; Madix, R. J. *J. Phys. Chem.* **1996**, *100*, 9807.
(83) Vasquez, N.; Muscat, A.; Madix, R. J. *Surf. Sci.* **1994**, *301*, 83.
(84) Gland, J. L.; Madix, R. J.; McCabe, R. W.; Demaggio, C. *Surf. Sci.* **1984**, *143*, 46.
(85) Johnson, S.; Madix, R. J. *Surf. Sci.* **1981**, *108*, 77.
(86) Bertolini, J. C.; Tardy, B. *Surf. Sci.* **1981**, *1981*, 131.
(87) Bertolini, J. C.; Dalmai-Imelik, G.; Rousseau, J. *Surf. Sci.* **1977**, *68*, 539.
(88) Diebold, U. *Appl. Phys. A* **2003**, *76*, 681.
(89) Henderson, M. A.; Epling, W. S.; Perkins, C. L.; Peden, C. H. F.; Diebold, U. *J. Phys. Chem. B* **1999**, *103*, 5328.
(90) Linsebigler, A.; Lu, G.; Yates, J. T. *J. Chem. Phys.* **1995**, *103*, 9438.
(91) Wang, L. Q.; Ferris, K. F.; Shultz, A. N.; Baer, D. R.; Engelhard, M. H. *Surf. Sci.* **1997**, *380*, 352.

(92) Henderson, M. A.; Szanyi, J.; Peden, C. H. F. *Catal. Today* **2003**, *85*, 251.
(93) Lu, G.; Linsebigler, A.; Yates, J. T. *J. Phys. Chem.* **1994**, *98*, 11733.
(94) Rodriguez, J. A.; Jirsak, T.; Liu, G.; Hrbek, J.; Dvorak, J.; Maiti, A. *J. Am. Chem. Soc.* **2001**, *123*, 9597.
(95) Henderson, M. A. *Langmuir* **1996**, *12*, 5093.
(96) Farfan-Arribas, E.; Madix, R. J. *Surf. Sci.* **2003**, *544*, 241.
(97) Tanner, R. E.; Liang, Y.; Altman, E. I. *Surf. Sci.* **2002**, *506*, 251.
(98) Berkó, A.; Bíró, T.; Solymosi, F. *J. Phys. Chem. B* **2000**, *104*, 2506.
(99) Ciuparu, D.; Bozon-Verduraz, F.; Pfefferle, L. *J. Phys. Chem. B* **2002**, *106*, 3434.
(100) Bennet, R. A.; Stone, P.; Smith, R. D.; Bowker, M. *Surf. Sci.* **2000**, *454*−*456*, 390.